Chemistry & Biology
Article

# Blockade of Inflammatory Responses by a Small-Molecule Inhibitor of the Rac Activator DOCK2

Akihiko Nishikimi,[1,2,5,10] Takehito Uruno,[1,10] Xuefeng Duan,[2] Qinhong Cao,[1] Yuji Okamura,[6] Takashi Saitoh,[3] Nae Saito,[7] Shunsuke Sakaoka,[6] Yao Du,[6] Atsushi Suenaga,[9] Mutsuko Kukimoto-Niino,[5,9] Kei Miyano,[4] Kazuhito Gotoh,[1,5] Takayoshi Okabe,[7] Fumiyuki Sanematsu,[1,2,5] Yoshihiko Tanaka,[1,2,5] Hideki Sumimoto,[4] Teruki Honma,[9] Shigeyuki Yokoyama,[5,8,9] Tetsuo Nagano,[6,7] Daisuke Kohda,[2,3] Motomu Kanai,[6] and Yoshinori Fukui[1,2,5,*]

[1]Division of Immunogenetics, Department of Immunobiology and Neuroscience, Medical Institute of Bioregulation
[2]Research Center for Advanced Immunology
[3]Division of Structural Biology, Medical Institute of Bioregulation
[4]Department of Biochemistry, Graduate School of Medical Sciences
Kyushu University, Fukuoka 812-8582, Japan
[5]Japan Science and Technology Agency, Core Research for Evolutional Science and Technology (CREST), Tokyo 102-0075, Japan
[6]Graduate School of Pharmaceutical Sciences
[7]Open Innovation Center for Drug Discovery
[8]Department of Biophysics and Biochemistry, Graduate School of Science
The University of Tokyo, Tokyo 113-0033, Japan
[9]RIKEN Systems and Structural Biology Center, Yokohama 230-0045, Japan
[10]These authors contributed equally to this work
*Correspondence: fukui@bioreg.kyushu-u.ac.jp
DOI 10.1016/j.chembiol.2012.03.008

## SUMMARY

**Tissue infiltration of activated lymphocytes is a hallmark of transplant rejection and organ-specific autoimmune diseases. Migration and activation of lymphocytes depend on DOCK2, an atypical Rac activator predominantly expressed in hematopoietic cells. Although DOCK2 does not contain Dbl homology domain typically found in guanine nucleotide exchange factors, DOCK2 mediates the GTP-GDP exchange reaction for Rac through its DHR-2 domain. Here, we have identified 4-[3′-(2″-chlorophenyl)-2′-propen-1′-ylidene]-1-phenyl-3,5-pyrazolidinedione (CPYPP) as a small-molecule inhibitor of DOCK2. CPYPP bound to DOCK2 DHR-2 domain in a reversible manner and inhibited its catalytic activity in vitro. When lymphocytes were treated with CPYPP, both chemokine receptor- and antigen receptor-mediated Rac activation were blocked, resulting in marked reduction of chemotactic response and T cell activation. These results provide a rational of and a chemical scaffold for development of the DOCK2-targeting immunosuppressant.**

## INTRODUCTION

Tissue infiltration of activated lymphocytes is a hallmark of transplant rejection and organ-specific autoimmune diseases (Gerard and Rollins, 2001; Luster et al., 2005). This process involves a complex cascade of molecular interactions and cellular responses, including the chemokine-dependent migration of lymphocytes, the recognition by T cell receptors (TCRs) of allo- or self-peptides bound to major histocompatibility complex (MHC) molecules, the engagement of costimulation and adhesion molecules with their ligands, and the activation of multiple intracellular signal transduction pathways that lead to the release of cytokines that are key to lymphocyte expansion and tissue destruction. Thus far, TCR signaling pathways have been the major targets for drug discovery, and the resultant calcineurin inhibitors, cyclosporine and FK506, successfully controlled allograft rejection in clinical and experimental transplantation (Denton et al., 1999). More recently, FTY720, which acts as a functional antagonist for sphingosine 1-phosphate receptor and inhibits lymphocyte egress from the secondary lymphoid organs, has been developed as a novel immunomodulatory drug (Brinkmann et al., 2010; Mandala et al., 2002). However, because both migration and activation of lymphocytes requires remodeling of the actin cytoskeleton (Dustin and Cooper, 2000; Vicente-Manzanares and Sánchez-Madrid, 2004), inhibition of the cytoskeletal reorganization in lymphocytes may be an alternative approach to control transplant rejection and organ-specific autoimmune diseases.

Rac is the small GTPase that regulates membrane polarization and cytoskeletal dynamics in varied biological settings (Hall, 1998). Like other small GTPases, Rac cycles between GDP-bound inactive and GTP-bound active states, and stimulus-induced formation of the active Rac is mediated by guanine nucleotide exchange factors (GEFs). The critical role of Rac activation in lymphocyte migration has been well established (Faroudi et al., 2010; Tybulewicz and Henderson, 2009). Moreover, the activation of Rac has been implicated in immunological synapse formation, a large-scale molecular movement at the interface between T cells and antigen presenting cells (APCs),

 

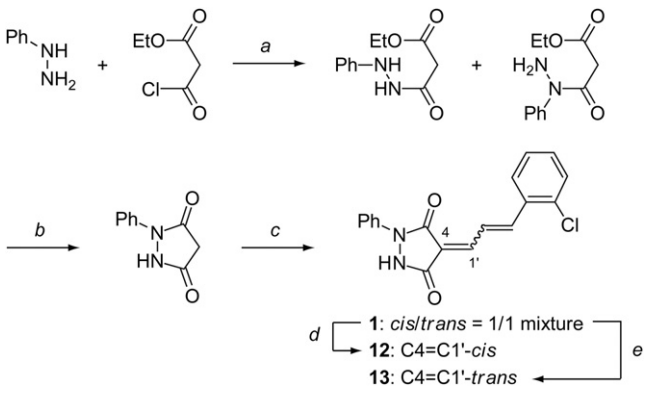


**Figure 1. Synthesis of CPYPP (1) and Its Geometrically Pure Isomers**
Reagents and conditions: a, $Et_3N$, THF, –10°C, 68%, 3:1 inseparable mixture; b, 1 M NaOH in EtOH, room temperature, 58%; c, 3-(2′-Chlorophenyl)propenal, proline (10 mol %), THF, room temperature, 70%; d, Wash with $CHCl_3$, 90%; e, $SiO_2$ medium-pressure column with AcOEt/hexanes = 2/5 elution. The synthesis and purification of CPYPP and its geometrically pure isomers (**12**, **13**) are described in Supplemental Experimental Procedures in detail.
See also Figure S1.

which is considered to be critical for sustained T cell activation (Dustin and Cooper, 2000; Villalba et al., 2001; Yu et al., 2001). Therefore, Rac activation would be a target to manipulate lymphocyte functions. However, Rac is composed of three isoforms, and the ubiquitous expression and redundancy of Rac isoforms preclude using Rac itself as a drug target.

DOCK2 is a member of the CDM family of proteins (*Caenorhabditis elegans* CED-5, mammals DOCK180, and *Drosophila melanogaster* Myoblast City) and is predominantly expressed in hematopoietic cells (Reif and Cyster, 2002). Although DOCK2 does not contain the Dbl homology (DH) domain and the Pleckstrin homology (PH) domain typically found in GEFs, DOCK2 catalyzes the GTP–GDP exchange reaction for Rac by means of its DHR-2 (DOCK homology region 2; also known as Docker and CZH2) domain (Brugnera et al., 2002; Côté and Vuori, 2002; Meller et al., 2002). DOCK2 is essential for chemokine receptor- and antigen receptor-mediated Rac activation, and plays a critical role in migration and activation of lymphocytes (Fukui et al., 2001; Nombela-Arrieta et al., 2004; Nombela-Arrieta et al., 2007; Sanui et al., 2003; Shulman et al., 2006). Consistent with the critical roles of DOCK2 in lymphocyte functions, DOCK2 deficiency enables long-term survival of cardiac allografts (Jiang et al., 2005) and abrogates development of autoimmune diabetes in NOD mice (our unpublished observation), a model for human type I diabetes (Anderson and Bluestone, 2005). Thus, DOCK2 may serve as a molecular target for controlling immune-related disorders.

Here, we report identification and characterization of a small-molecule, 4-[3′-(2″-chlorophenyl)-2′-propen-1′-ylidene]-1-phenyl-3,5-pyrazolidinedione (CPYPP). We found that CPYPP binds to the DOCK2 DHR-2 domain ($DOCK2^{DHR\text{-}2}$) in a reversible manner and inhibits its catalytic activity. Although overexpression of DOCK2, Tiam1, or Trio induced Rac activation in human embryonic kidney 293T (HEK293T) cells, CPYPP suppressed DOCK2-mediated Rac activation, without affecting Rac activation by the classical GEFs. More importantly, treatment of lymphocytes with CPYPP blocked DOCK2-mediated Rac activation and inflammatory responses in vitro and in vivo. Our results thus provide a rational of and a chemical scaffold for development of the DOCK2-targeting immunosuppressant.

## RESULTS

### Identification of CPYPP as a Small-Molecule Inhibitor of DOCK2

DOCK2 binds to Rac through its DHR-2 domain and mediates GTP–GDP exchange reaction (Brugnera et al., 2002; Côté and Vuori, 2002). Therefore, this interaction would be the first target to block DOCK2-mediated inflammatory responses. We screened 9,392 chemical compounds in terms of their ability to inhibit interaction between $DOCK2^{DHR\text{-}2}$ and Rac1 (see Table S1 available online), and identified 131 candidates including CPYPP (compound **1**; Figures 1 and 2A). CPYPP inhibited the GEF activity of $DOCK2^{DHR\text{-}2}$ for Rac1 in a dose-dependent manner, with a half-maximal inhibitory concentration ($IC_{50}$) of 22.8 ± 2.4 μM (Figure 2B). This inhibitory activity was independent on length of preincubation time, ranging from 2 min to 30 min (Figure S2). In addition, CPYPP was nontoxic when applied to spleen cells or thymoma cells (BW5147$\alpha^-\beta^-$) at 100 μM for 3 hr or 3 days, respectively (Figure S2). Then, CPYPP was selected and synthesized in gram-scales for further evaluation (Figures 1 and S1).

Recent structure of $DOCK2^{DHR\text{-}2}$ complexed with Rac (Kulkarni et al., 2011) indicates that the DHR-2 domain of DOCK2 is also organized into three lobes (lobes A, B, and C), as in DOCK9 DHR-2 (Yang et al., 2009). Deletion of the amino acid sequence corresponding to the lobe A (residues 1,195–1,335) in $DOCK2^{DHR\text{-}2}$ did not affect its GEF activity in vitro (Figure 2B), indicating that Rac binding site and catalytic center are generated entirely from lobes B and C. As expected, Rac1 activation by this mutant ($DOCK2^{DHR\text{-}2\Delta lobeA}$) was also inhibited by CPYPP in vitro, although the $IC_{50}$ value was a little bit higher than that for wild-type $DOCK2^{DHR\text{-}2}$ (Figure 2B). To determine whether CPYPP binds to DHR-2 or Rac1, we utilized saturation transfer difference (STD)-nuclear magnetic resonance (NMR) spectroscopy (Meyer and Peters, 2003), which allows detection of weak ligand binding by revealing the spatial proximity between ligand protons and protein protons. Protein concentration used was 1 μM, and the ligands were added in 100-fold molar excess. Therefore, only the ligand $^1H$ signals were observed in the STD spectra, and the protein $^1H$ signals were invisible with the assistance of the suppressive effect of the T1ρ filter in the NMR pulse sequence. By irradiation of the methyl region of the spectrum, all of the $^1H$ signals of CPYPP showed the same degree of reduction in intensity (average, –23%) in the presence of the $DOCK2^{DHR\text{-}2\Delta lobeA}$ (Figure 2C). In contrast, no significant difference was observed when CPYPP was mixed with Rac1 (Figure 2C). Thus, CPYPP inhibits Rac GEF activity of DOCK2 by binding to the DHR-2 domain.

DOCK proteins are classified into four subfamilies (DOCK-A, -B, -C, and -D) based on their structures and substrate specificity (Côté and Vuori, 2002). For example, DOCK180 and DOCK5, as well as DOCK2, belong to DOCK-A subfamily and act as Rac GEFs. On the other hand, DOCK9, a member of DOCK-D subfamily, catalyzes Cdc42 activation through its

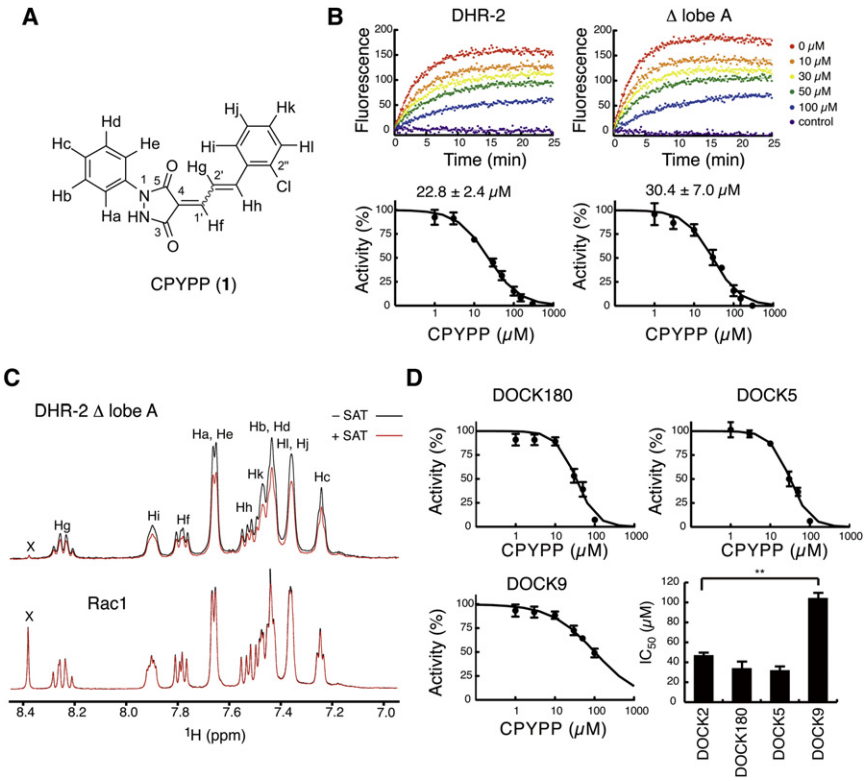


**Figure 2. CPYPP Inhibits Rac GEF Activity of DOCK2 through Interaction with DHR-2 Domain**

(A) Structure of CPYPP. Ha-Hl correspond to the $^1$H spectra in (C).

(B) Concentration-dependent inhibition by CPYPP of in vitro GEF activity of DOCK2$^{DHR-2}$ with or without lobe A. Dose response curves and $IC_{50}$ values (mean ± SD of three independent experiments) are shown in lower panels.

(C) The STD-NMR analysis showing that CPYPP binds to DOCK2$^{DHR-2}$, but not to Rac. The expanded region of the 1D $^1$H NMR spectra of CPYPP with (+SAT) or without (–SAT) saturation of the protein signals of DOCK2$^{DHR-2\Delta lobeA}$ or Rac1. The impurity peak is denoted by x.

(D) Comparison of inhibitory activity of CPYPP among DOCK family proteins. The DHR-2 domain lacking lobe A was prepared from each molecule and analyzed for its GEF activity toward Rac (DOCK2, DOCK180, and DOCK5) or Cdc42 (DOCK9) in the presence of various concentrations of CPYPP. Graph shows $IC_{50}$ values (mean ± SD of three independent experiments) for each protein. **p < 0.01.

See also Figure S2 and Table S1.

DHR-2 domain (Meller et al., 2002). To address the specificity of CPYPP, we compared the effect of CPYPP on the GEF activity of these DOCK proteins in vitro. CPYPP inhibited the Rac GEF activity of DOCK180$^{DHR-2\Delta lobeA}$ and DOCK5$^{DHR-2\Delta lobeA}$ with the $IC_{50}$ value comparable to that for DOCK2$^{DHR-2\Delta lobeA}$ (Figure 2D). However, CPYPP was much less effective in inhibition of DOCK9$^{DHR-2\Delta lobeA}$-mediated Cdc42 activation (Figure 2D). These results indicate that, although the inhibitory effect of CPYPP is not specific to DOCK2, CPYPP is able to discriminate the structural difference among DOCK subfamily members.

## Structural Features of CPYPP

To determine the structure of CPYPP required for its inhibitory effect, we synthesized CPYPP analogs (Figures 3A and S1) and compared their effects on the Rac GEF activity of DOCK2$^{DHR-2}$ in vitro. When the double bonds were saturated through hydrogenation in compound **2**, the inhibitory activity was markedly decreased (Figure 3B). In contrast, both compound **3** with one double bond and compound **4** with three double bonds inhibited DOCK2-mediated Rac activation with $IC_{50}$ values comparable to that of CPYPP with two double bonds (Figure 3C). Thus, at least one double bond is essential for the inhibitory activity of CPYPP. Another important feature of CPYPP would be a chloride substituent at the ortho (2″)-position of an aryl group on the conjugated double bonds. We found that the inhibitory activity was significantly suppressed in nonsubstituted compound **5** and compounds **6**–**9** with hydroxy, fluoride, bromide, and methyl groups, respectively, at the ortho-position (Figure 3C). However, the position of the chloride group on the aromatic ring did not critically affect the inhibitory activity (Figures 3A and 3C; see compounds **10** and **11**).

The importance of the electron-deficient double bonds in CPYPP may raise the possibility that its inhibitory effect is mediated by covalent adducts via Michael addition. To address this possibility, we analyzed the binding of CPYPP to DOCK2$^{DHR-2\Delta lobeA}$ using a surface plasmon resonance (SPR)-based instrument. Although compound **7** with fluoride at the ortho-position did not show any binding to DOCK2$^{DHR-2\Delta lobeA}$, CPYPP bound to DOCK2$^{DHR-2\Delta lobeA}$ in a reversible manner (Figure 3D). In addition, we found that DOCK2$^{DHR-2}$ treated with CPYPP normally retained the GEF activity after removable of CPYPP by gel filtration (Figure S3). These results indicate that inhibition by CPYPP is reversible.

CPYPP and all the analogs exist as hardly separable equilibrium mixtures (1:1 to 1.6:1) of two geometrical isomers at the C4=C1′ double bond (Figure 4A). *Cis* isomer **12** is less soluble to various organic solvents than *trans* isomer **13**, allowing for isolation of *cis* isomer **12** as a pure solid form by washing a mixture with chloroform for several times. On the other hand, *trans* isomer **13** was isolated by medium-pressure silica gel column chromatography. The configuration of **12** and **13** was determined from the comparison of the two coupling constants, $^3J_{C3\text{-}H1'}$ and $^3J_{C5\text{-}H1'}$ across the C4=C1′ double bond (Figure S4). Isolated **12** and **13** readily equilibrated each other when dissolved in solution (such as DMSO, methanol, and acetone) at ambient temperature, giving a 1:1 mixture of two isomers. Even so, isolated **12** and **13** were quickly subjected to the Rac GEF activity assay to obtain preliminary information about the double bond geometry-activity relationship. As a result, *cis* isomer **12** exhibited slightly higher activity than CPYPP (1:1 mixture of **12** and **13**), whereas *trans* isomer **13** did not show any inhibitory activity (Figure 4B). These results

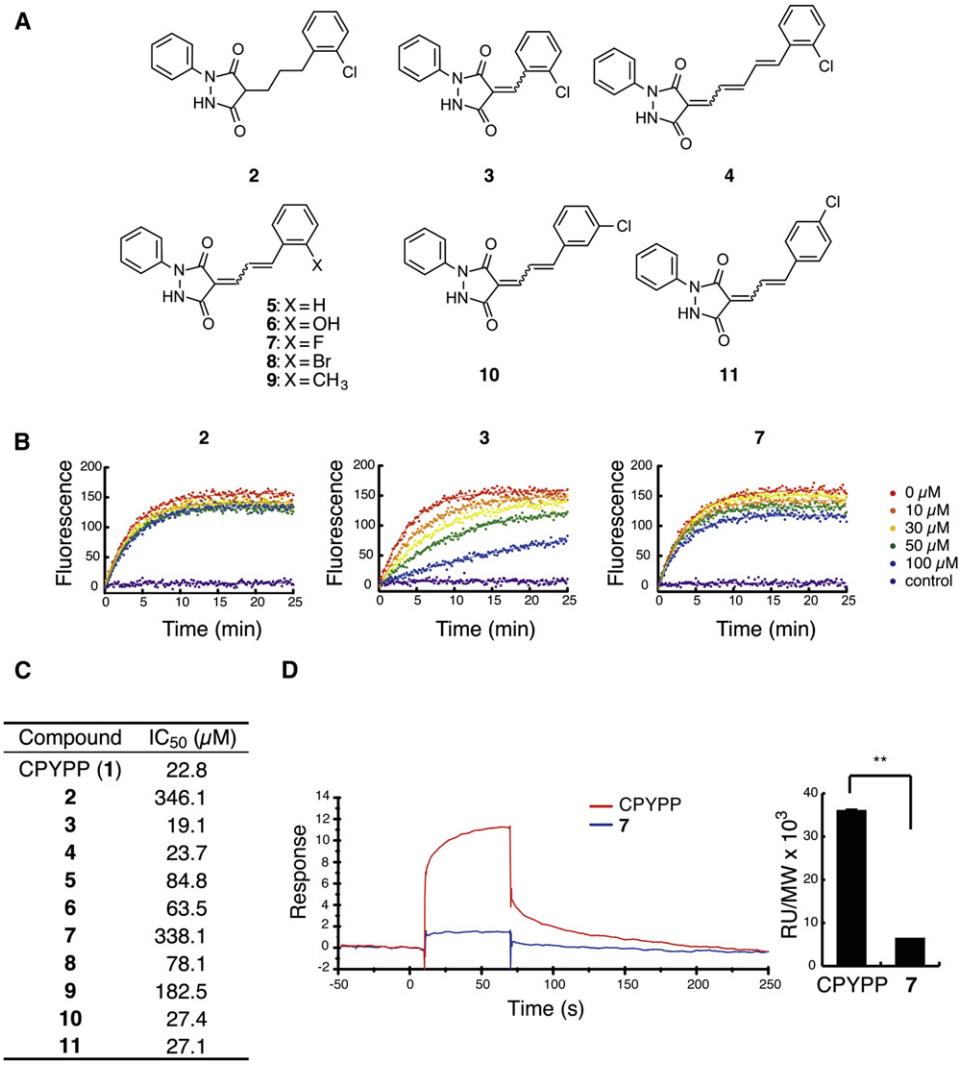


| Compound | $IC_{50}$ ($\mu$M) |
|---|---|
| CPYPP (**1**) | 22.8 |
| **2** | 346.1 |
| **3** | 19.1 |
| **4** | 23.7 |
| **5** | 84.8 |
| **6** | 63.5 |
| **7** | 338.1 |
| **8** | 78.1 |
| **9** | 182.5 |
| **10** | 27.4 |
| **11** | 27.1 |

**Figure 3. Structure-Activity Relationship of CPYPP**

(A) CPYPP analogs used in this study (**2**–**11**).

(B) Importance of the conjugated double bonds and the chloride substituent for the inhibitory activity of CPYPP. Rac GEF activity of $DOCK2^{DHR-2}$ was analyzed in vitro in the presence of compounds **2**, **3**, or **7**.

(C) Comparison of $IC_{50}$ values for $DOCK2^{DHR-2}$-mediated Rac GEF activity among CPYPP analogs.

(D) SPR-based analysis showing that CPYPP, but not compound **7**, binds to $DOCK2^{DHR-2\Delta lobeA}$ in a reversible manner. The graph indicates the response levels normalized by dividing the measured response units by the molecular weight. Data are mean ± SD of three independent experiments. $^{**}p < 0.01$.

See also Figure S3.

suggest that the inhibitory activity of CPYPP resides in *cis* isomer.

## CPYPP Is a Cell-Active Inhibitor of DOCK2

To examine whether CPYPP is a cell-active inhibitor, we expressed DOCK2 in HEK293T cells, and analyzed Rac activation in the presence or absence of CPYPP. Although overexpression of DOCK2 induced Rac activation in HEK293T cells, this activation was markedly suppressed by treating the cells with CPYPP (**1**) at 100 μM for 1 hr before assay (Figure 5A). Similar inhibition was obtained when HEK293T cells were treated with CPYPP analogs such as **3**, **10**, or **11** (Figure 5A), all of which exhibited $IC_{50}$ values <30 μM in vitro (Figure 3C). Indeed, except for compounds **4** and **6**, the $IC_{50}$ values were well correlated to the degrees of inhibition of DOCK2-mediated Rac activation in HEK293T cells (Figure 5A). On the other hand, treatment with CPYPP did not significantly inhibit Rac activation by Tiam1 and Trio under the same experimental condition (Figure 5B). These results indicate that CPYPP is able to distinguish DOCK2 from the Dbl-like GEFs and inhibit DOCK2-mediated Rac activation in cells.

## Inhibition by CPYPP of Lymphocyte Migration

To examine whether CPYPP inhibits DOCK2-dependent lymphocyte functions, we first analyzed the effect of CPYPP on chemokine-induced Rac activation. As previously reported

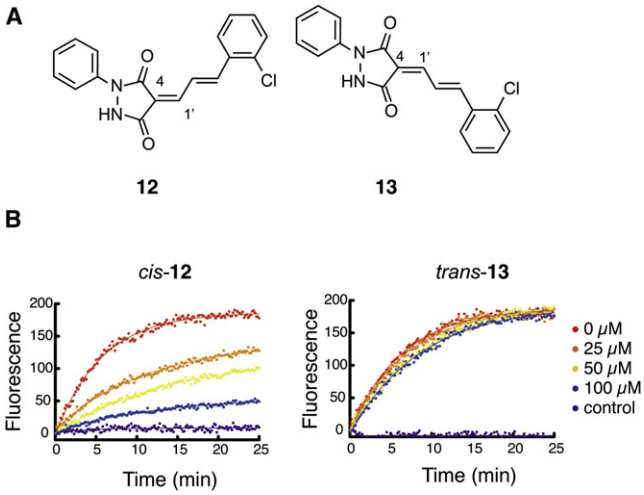


**Figure 4. Inhibitory Activity of CPYPP Resides in *cis* Isomer**

(A) Structure of *cis* (**12**) and *trans* (**13**) isomers of CPYPP.

(B) The effect of *cis* and *trans* isomers on in vitro Rac GEF activity. Upon isolation, *cis* and *trans* isomers of CPYPP were quickly subjected to in vitro GEF assays.

See also Figure S4.

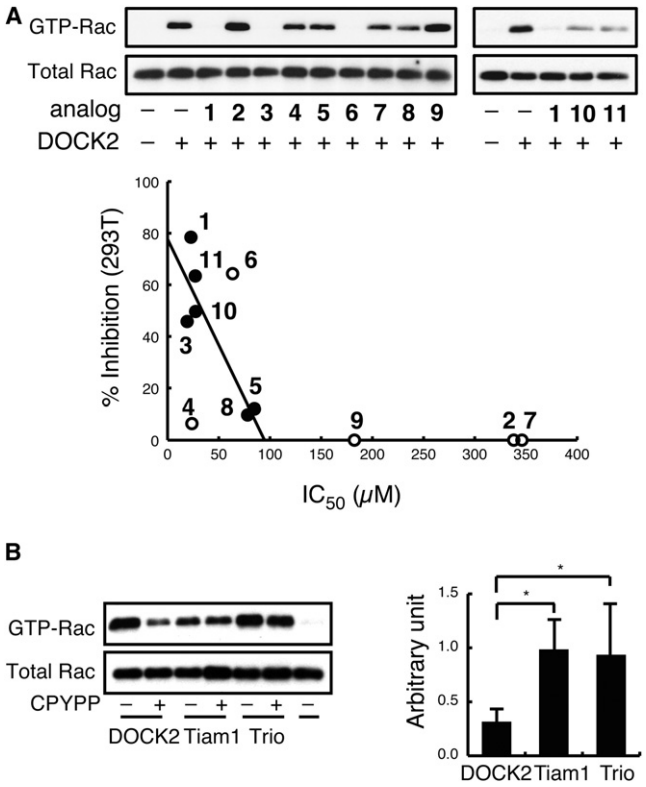


**Figure 5. CPYPP Is a Cell-Active Inhibitor of DOCK2**

(A) Comparison of inhibitory activity of CPYPP and its analogs for DOCK2-mediated Rac activation in HEK293T cells. The correlation coefficient between $IC_{50}$ values and the percentage inhibition (mean of three independent experiments) was 0.80. Compounds **4** and **6**, and inactive compounds (**2**, **7**, and **9**) that are excluded from the calculation are expressed as open circles.

(B) Selective inhibition by CPYPP of DOCK2-mediated Rac activation in HEK293T cells. Results are expressed as the ratio of GTP-bound Rac to total Rac after normalization of the value of DMSO-treated cells to an arbitrary unit 1 for each GEF. Data are mean ± SD of four independent experiments. *$p < 0.05$.

(Fukui et al., 2001), chemokine-induced Rac activation was severely impaired in DOCK2 deficient ($DOCK2^{-/-}$) T and B cells, indicating that this process is largely dependent on DOCK2 (Figures 6A and 6B). Although vehicle (DMSO) alone did not show any inhibitory effect, pretreatment of T cells or B cells with CPYPP at 100 μM for 1 hr markedly suppressed Rac activation in response to CCL21 or CXCL13, respectively (Figures 6A and 6B). Consistent with this finding, treatment with CPYPP effectively inhibited migratory response of T cells and B cells to these chemokines in a dose-dependent manner (Figures 6C and 6D). Lymphocytes also express DOCK5 (our unpublished observation). When CPYPP was applied to $DOCK2^{-/-}$ lymphocytes, their migration defects were further augmented (Figures 6C and 6D), probably because of the cross-reactivity of CPYPP to DOCK5.

To examine whether the effect of CPYPP could be extended to in vivo situation, we first tested administration route and dosage of CPYPP by measuring its plasma concentration using liquid chromatography-tandem mass spectrometry (LC-MS/MS). When 2.5 mg/kg of CPYPP was administrated intravenously, the plasma concentration of CPYPP was only 2.4 μM at 30 min (Figure S5). However, by intraperitoneally injecting 250 mg/kg of CPYPP into mice, the plasma concentration of CPYPP reached to 11.3 μM at 30 min and 10.9 μM at 1 hr, respectively (Figure S5). With this dose and administration route, we examined the effect of CPYPP on lymphocyte homing in vivo. For this purpose, we adoptively transferred spleen cells from mice that had been made by a "knock-in" strategy to express endogenous DOCK2 as a fusion protein with green fluorescent protein (GFP) (Nishikimi et al., 2009). Without pretreatment with CPYPP, 0.19% of the injected T cells, on an average, migrated to the peripheral lymph nodes of the recipient mice (Figure 6E). However, intraperitoneal injection of CPYPP (5 mg per mouse) 1 hr before adoptive transfer reduced the percentage of the migrated T cells to <25% of the control level (Figure 6E). Similar, but less remarkable effect, was observed when T cell homing to the spleen was analyzed (Figure 6E). On the other hand, intravenous injection of 0.05 mg of CPYPP did not show any inhibitory effect on lymphocyte homing in vivo (Figure 6E).

## Inhibition by CPYPP of Leukocyte Activation

Having found that CPYPP inhibits migratory response of lymphocytes, we next examined the effect of CPYPP on T cell activation. DOCK2 is a major Rac GEF acting downstream of TCRs (Sanui et al., 2003). Consistent with this, TCR-mediated Rac activation was almost completely lost in T cells treated with CPYPP at 100 μM for 1 hr (Figure 7A). $CD4^+$ T cells from C57BL/6 mice vigorously proliferated when cultured for 3 days with APCs from B10.BR mice (Figure 7B). However, this mixed lymphocyte reaction (MLR) was blocked by cultivating $CD4^+$ T cells and APCs in the presence of CPYPP at the concentration of 12.5 μM (Figure 7B). This assay was performed in complete

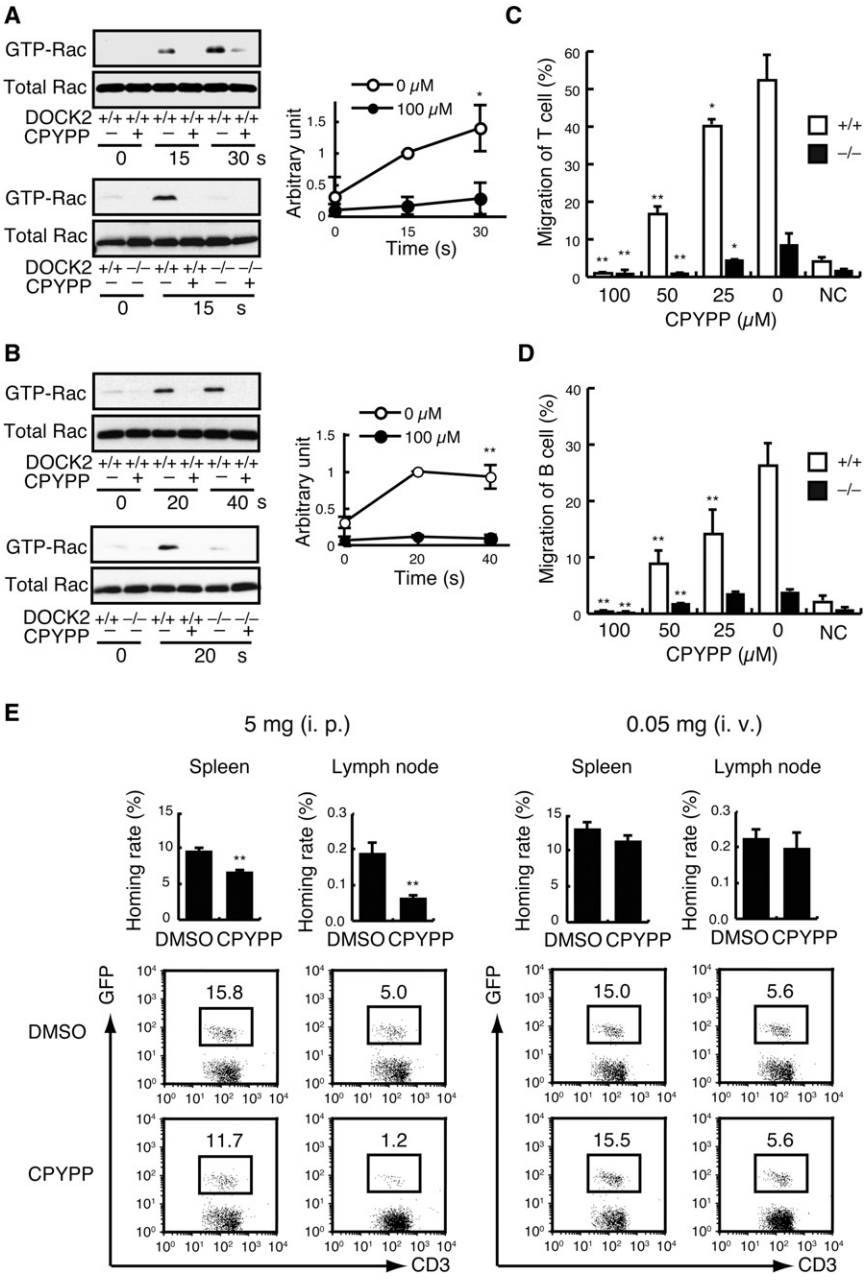


**Figure 6. CPYPP Blocks Lymphocyte Migration In Vitro and In Vivo**

(A and B) The effect of CPYPP on Rac activation in WT and DOCK2$^{-/-}$ T cells (A) or B cells (B) stimulated with CCL21 or CXCL13, respectively. Results are expressed as the ratio of GTP-bound Rac to total Rac after normalization of the 15 s (A) or 20 s (B) value of DMSO-treated cells to an arbitrary unit 1. Data are mean ± SD of three independent experiments.

(C and D) Inhibition by CPYPP of migratory response of WT and DOCK2$^{-/-}$ T cells (C) or B cells (D) to CCL21 or CXCL13, respectively. NC, no chemokine stimulation. Data are mean ± SD of triplicate samples and are representative of three independent experiments.

(E) Suppression of lymphocyte homing to secondary lymphoid organs in mice treated with CPYPP. Numbers in dot plots indicate the percentage of GFP$^+$ cells in CD3$^+$ T cells. In graphs, results are expressed as the percentage of migrated T cells to total injected T cells. Data are mean ± SEM of mice treated with CPYPP intraperitoneally (i.p.; 5 mg per mouse; n = 9) or intravenously (i.v.; 0.05 mg per mouse; n = 4), and are representative of two independent experiments. (A–E) *p < 0.05; **p < 0.01.

See also Figure S5.

RPMI1640 medium supplemented with 10% fetal calf serum (FCS), whereas the effect of CPYPP on lymphocyte migration was examined in RPMI1640 medium containing 0.5% bovine serum albumin (BSA). Because CPYPP was more effective in MLR than in migration assay (see Figure 6C), the efficiency of CPYPP uptake by lymphocytes might be different between these culture conditions. Indeed, we found that the intracellular content of CPYPP was much higher when splenocytes were incubated with CPYPP in complete RPMI1640 medium supplemented with 10% FCS (Figure S6).

By recognizing nucleic acid ligands through TLR7 and TLR9, pDCs produce not only inflammatory cytokines, but also large amounts of type I IFNs (Gilliet et al., 2008). This type I IFN induction has been implicated in the pathogenesis of certain autoimmune diseases such as psoriasis and systemic lupus erythematosus (Blanco et al., 2001; Nestle et al., 2005). Because DOCK2–Rac axis is critical in pDCs for TLR-mediated induction of type I IFNs, but not inflammatory cytokines (Gotoh et al., 2010), we also examined the effect of CPYPP on pDC activation. When pDCs were stimulated with A-type CpG DNA, a TLR9 ligand, activated Rac was readily detected (Figure 7C). However, treatment with CPYPP severely impaired CpG-A-induced Rac activation in pDCs (Figure 7C), resulting in loss of IFN-α induction without affecting IL-12p40 levels (Figure 7D). Collectively, these results indicate that treatment with CPYPP faithfully reproduces DOCK2-deficient phenotypes in lymphocytes and pDCs.

## DISCUSSION

Rac is an important signaling molecule that controls diverse cellular functions, including migration and activation of lymphocytes (Faroudi et al., 2010; Hall, 1998; Tybulewicz and Henderson, 2009; Villalba et al., 2001; Yu et al., 2001). Thus far, several chemical inhibitors acting at different steps of Rac signaling have been identified. For example, NSC23766 or EHT 1864 inhibits Rac activation by binding to Rac to compete with the GEF binding or to destabilize the bound nucleotide, respectively

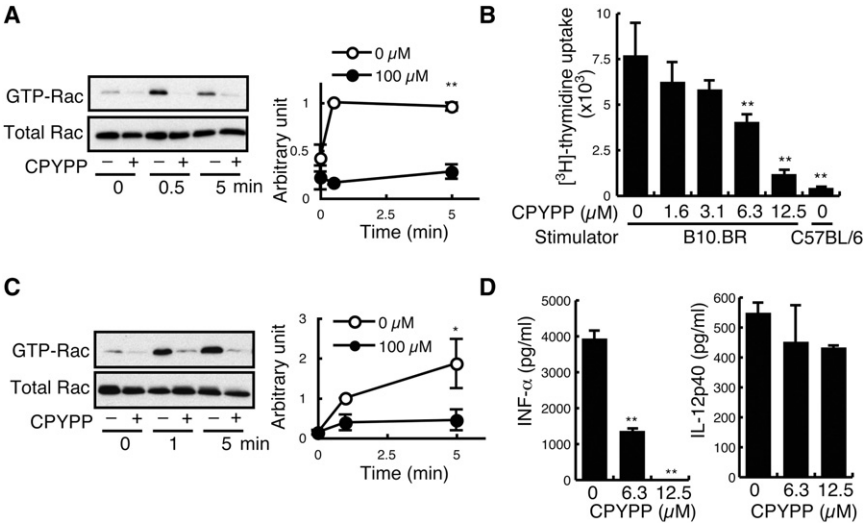


**Figure 7. CPYPP Blocks Activation of T Cells and pDCs**

(A) Inhibition by CPYPP of Rac activation in T cells stimulated with anti-CD3ε antibody. Results are expressed as the ratio of GTP-bound Rac to total Rac after normalization of the 0.5-min value of DMSO-treated cells to an arbitrary unit 1. Data are mean ± SD of three independent experiments.

(B) Inhibition by CPYPP of MLR between C57BL/6 and B10.BR mice. Data are mean ± SD of triplicate samples and are representative of three independent experiments.

(C) Inhibition by CPYPP of Rac activation in pDCs stimulated with CpG-A. Results are expressed as the ratio of GTP-bound Rac to total Rac after normalization of the 1-min value of DMSO-treated cells to an arbitrary unit 1. Data are mean ± SD of three independent experiments.

(D) Inhibition by CPYPP of TLR9–mediated type I IFN induction in pDCs. Data are mean ± SD of triplicate samples and are representative of three independent experiments. (A–D) *$p < 0.05$; **$p < 0.01$.

See also Figure S6.

(Gao et al., 2004; Shutes et al., 2007). On the other hand, IPA-3 is an inhibitor targeting p21-activated kinase (PAK), a downstream effector of Rac (Deacon et al., 2008). However, because Rac and PAK isoforms are expressed in many cell-types, they are not ideal targets to control immune responses. Unlike these molecules, DOCK2 expression is limited to hematopoietic cells (Fukui et al., 2001). More importantly, DOCK2 is a Rac activator essential for migration and activation of lymphocytes (Fukui et al., 2001; Nombela-Arrieta et al., 2004, 2007; Sanui et al., 2003; Shulman et al., 2006), and its deficiency has been demonstrated to suppress allograft rejection and autoimmune disease development (Jiang et al., 2005). Therefore, DOCK2 may serve as a better therapeutic target for controlling immune-related disorders.

Here, we have identified CPYPP as a small-molecule inhibitor of DOCK2. CPYPP bound to DOCK2$^{DHR-2}$ and inhibited its Rac GEF activity with $IC_{50}$ of 22.8 μM. Unfortunately, CPYPP was not specific to DOCK2 and showed cross-reactivity to other DOCK-A members, DOCK5 and DOCK180. However, CPYPP inhibited DOCK2-mediated Rac activation, without affecting Rac activation by Tiam1 and Trio. Thus, CPYPP is a selective inhibitor that can distinguish DOCK2 from the classical GEFs. Although CPYPP is a potentially reactive Michael acceptor, the SPR-based analysis indicated that CPYPP binds to DOCK2$^{DHR-2}$ in a reversible manner. Indeed, when CPYPP was treated with 2-mercaptoethanol (1 equivalent) in the assay buffers in the presence of BSA for 1 hr, CPYPP was recovered quantitatively in intact form without Michael reaction (our unpublished observation). In addition, we confirmed that the DOCK2$^{DHR-2}$ treated with CPYPP is functionally reversible. Therefore, inhibitory activity of CPYPP is not due to covalent modification of DOCK2.

CPYPP and its analogs can be readily synthesized in practical scales. The synthetic route includes convergent Knoevenagel condensation between aldehydes and pyrazolidinediones, allowing for rapid supply of structurally diverse analogs of CPYPP. Current structure–activity relationship studies clarified the critical importance of the electron-deficient double bonds in the compounds, conjugated to the two carbonyl groups of the pyrozolidinedione part, for their binding and inhibitory activities. This result suggests the existence of critical hydrophobic interactions between the inhibitor's electron-deficient π-orbitals and the binding pocket of DOCK2$^{DHR-2}$. Additionally, the molecular flatness of compounds **1**, **3**, and **4**, compared with **2** containing $sp^3$ carbons, would also contribute to their binding ability. On the other hand, effects of the substituents on the aromatic ring at the conjugated diene moiety on the inhibitory activity are more difficult to rationalize. An ortho-substituent with an appropriate size and electron-withdrawing ability (such as *o*-chloride containing **1**) seems to be beneficial for the inhibitory activity. If a chloride substituent exists, however, its position on the aromatic ring is not very critical (**1**, **10**, and **11**). This result may also support the importance of the electronic characteristics of inhibitors' π-orbitals for their interaction with DOCK2$^{DHR-2}$.

We also elucidated the *cis*-geometry of C4=C1′ double bond in CPYPP as an additional structural requirement for the inhibitory activity. Because the double bond geometry was labile and readily equilibrated each other in a solution state, pure isomers were hardly separable. However, we fortunately found that the active *cis*-isomer **12** could be conveniently isolated in a gram scale through crystallization. The olefin geometry is stable in a solid state. In addition, *trans*-isomer **13** was isolated in a sub-mg scale by silica gel column chromatography. Comparison of the inhibitory activity between **12** and **13** demonstrated that the inhibitory activity resides in the *cis*-isomer **12**. Therefore, DOCK2$^{DHR-2}$ differentiates bent (*cis*) or linear (*trans*) global structure of CPYPP.

Although calcineurin inhibitors such as cyclosporine and FK506 have been successfully used to prevent "unwanted" immune responses, development of novel immunosuppressants with different actions is required to reduce their side effects. In this respect, DOCK2 also would be a good drug target, because DOCK2 deficiency has been demonstrated to synergistically act with FK506 in controlling transplant rejection (Jiang et al.,

2005). Consistent with the role of DOCK2 as a master regulator for Rac activation in lymphocytes, treatment with CPYPP almost completely abolished chemokine receptor- and TCR-mediated Rac activation in lymphocytes, resulting in marked reduction of chemotactic response and T cell activation. In addition, we found that TLR9-mediated IFN-$\alpha$ induction is selectively inhibited in pDCs treated with CPYPP. These results indicate that CPYPP is able to block effectively DOCK2-mediated inflammatory responses. Therefore, pharmacological inhibition of DOCK2 could be an attractive therapeutic strategy for controlling immune-related disorders, such as autoimmune diseases and transplant rejection, caused by tissue infiltration of activated lymphocytes. Design and synthesis of geometrically constrained molecules with the electronic and structural properties identified in this study will lead to development of more potent and more selective DOCK2 inhibitors that can be used as a drug lead.

## SIGNIFICANCE

**DOCK2, a mammalian homolog of *Caenorhabditis elegans* CED-5 and *Drosophila melanogaster* Myoblast city, is an atypical Rac activator predominantly expressed in hematopoietic cells. Although DOCK2 does not contain Dbl homology domain typically found in guanine nucleotide exchange factors (GEFs), DOCK2 mediates the GTP-GDP exchange reaction for Rac through its DHR-2 domain. DOCK2 plays a key role in migration and activation of lymphocytes, and its deficiency suppresses allograft rejection and autoimmune disease development in mice. Therefore, DOCK2 may serve as a molecular target for controlling immune-related disorders. Here, we have identified 4-[3′-(2″-chlorophenyl)-2′-propen-1′-ylidene]-1-phenyl-3,5-pyrazolidinedione (CPYPP) as a small-molecule inhibitor of DOCK2. CPYPP bound to DOCK2 DHR-2 domain in a reversible manner and inhibited its catalytic activity, without affecting Rac activation by the classical GEFs. The structure–activity relationship study revealed the importance of the electron-deficient double bonds, a chloride substituent on the aromatic ring, and the *cis*-geometry for inhibitory activity of CPYPP. When lymphocytes were treated with CPYPP, both chemokine receptor- and antigen receptor-mediated Rac activation were blocked, resulting in marked reduction of chemotactic response and T cell activation. These results suggest that pharmacological inhibition of DOCK2 could be a therapeutic strategy for controlling immune-related disorders, and provide a rational of and a chemical scaffold for development of the DOCK2-targeting immunosuppressant.**

## EXPERIMENTAL PROCEDURES

### Chemical Compounds

A total of 9,392 chemical compounds used for the initial screening were obtained from Open Innovation Center for Drug Discovery at The University of Tokyo, Japan. The synthesis and purification of CPYPP and its analogs are described in Supplemental Experimental Procedures in detail. Compounds were dissolved in DMSO, and diluted with appropriate buffers immediately before use. The percentage of DMSO used for cellular assays or in vitro GEF assay was 0.2% or 1%, respectively.

### Plasmids

For expression of DOCK2, Tiam1, or Trio DH-D1/PH-D1 domain in mammalian cells, their cDNAs were amplified by PCR with primers encoding hemagglutinin (HA) tag, and cloned into pCI (Promega) or pcDNA-His/max (Invitrogen). The pET-SUMO vector was created by subcloning SUMO cDNA into pET-28a vector (Novagen). The genes encoding $DOCK2^{DHR\text{-}2}$, $DOCK2^{DHR\text{-}2\Delta lobeA}$, $DOCK180^{DHR\text{-}2\Delta lobeA}$, $DOCK5^{DHR\text{-}2\Delta lobeA}$, and $DOCK9^{DHR\text{-}2\Delta lobeA}$ were cloned into the pET-SUMO to express fusion proteins with His tag at their N terminus, which were used for in vitro GEF assays, STD-NMR assays, and SPR-based binding assays. For screening of chemical compounds, $DOCK2^{DHR\text{-}2}$ with trigger factor (TF) at the N terminus and streptavidin binding protein (SBP) at the C terminus was created using pET-22b vector. The gene encoding Rac1 or Cdc42 was cloned into pGEX-6P-1 (GE Healthcare) to express glutathione-S-transferase (GST)-fusion protein.

### Screening of Chemical Library

An ELISA was employed to screen for chemical compounds that can inhibit interaction between $DOCK2^{DHR\text{-}2}$ and Rac. Briefly, 96-well polystyrene plates were coated overnight with streptavidin (250 ng per well) dissolved in 50 mM carbonate buffer (pH 9.6). Each well was blocked with 150 μl of 5% skim milk in TBST (20 mM Tris-HCl, 150 mM NaCl, 0.1% Tween-20, pH7.5) at room temperature for 1 hr. After the wells were rinsed with TBST, recombinant TF-$DOCK2^{DHR\text{-}2}$-SBP (50 μl, 60 μg/ml in TBST) was added to each well and incubated at room temperature for 1 hr. The wells were then rinsed with TBST supplemented with 1 mM EDTA. To each well, the library component or vehicle (50 μl, 200 μM in TBST/1 mM EDTA/2% DMSO) was added and incubated at room temperature for 1 hr. After incubation, GST-Rac1 or GST-Cdc42 (50 μl, 50 μg/ml in TBST/1 mM EDTA) was added to each well and incubated for 1 hr at room temperature. The wells were then rinsed with 150 μl of TBST/1 mM EDTA. Horseradish peroxidase-conjugated anti-GST antibody (50 μl, in TBST/1 mM EDTA) wad added to each well and incubated for 1 hr at room temperature. After the wells were rinsed with TBST/1 mM EDTA, peroxidase substrate (50 μl, 0.4 mg/ml *o*-phenylenediamine and 0.01% $H_2O_2$ in 0.1 M citrate buffer, pH 5.0) was added to each well and incubated for 30–60 min at room temperature. The absorbance was measured at 450 nm with a Multiskan Bichromatic plate reader (Labsystems) and compensated by subtracting "blank" absorbance of the well into which GST-Cdc42 was added. Percent inhibition was calculated as follows: [(optical density with vehicle alone) – (optical density with sample)]/(optical density with vehicle alone) × 100. Compounds were regarded as potential hits if they had an inhibitory effect >40%.

### Mice

$DOCK2^{-/-}$ and DOCK2-GFP knock-in mice have been described previously (Fukui et al., 2001; Nishikimi et al., 2009). All mice were maintained under specific pathogen-free conditions in the animal facility of Kyushu University. Animal protocols were approved by the committee of Ethics on Animal Experiment, Faculty of Medical Sciences, Kyushu University.

### In Vitro GEF Assays

Recombinant GEF protein diluted in exchange buffer (20 mM MES-NaOH, 150 mM NaCl, 10 mM $MgCl_2$, 0.2 mg/ml BSA, 20 μM GDP, pH 7.0) was incubated with chemical compounds or DMSO (vehicle) for 2–30 min in the dark at room temperature. Unbound CPYPP was removed using a spin column gel filtration (Edge Bio) at this stage when the functional reversibility of $DOCK2^{DHR\text{-}2}$ was analyzed. Recombinant Rac or Cdc42 (15 μM) was loaded with GDP in the same reaction buffer on ice for 30 min. GDP-loaded G-proteins (100 μl) were allowed to equilibrate in exchange buffer supplemented with *N*-methylanthraniloyl (mant)-GTP (3.6 μM; Jena Bioscience) or BODIPY-FL-GTP (3.6 μM; Invitrogen) for 8 min. After equilibration, pretreated GEF (50 μl) was added to the mixtures and the change of mant-GTP fluorescence (excitation = 360 nm, emission = 440 nm) or BODIPY-FL fluorescence (excitation = 488 nm, emission = 514 nm) was monitored at 30°C using a XS-N spectrofluorimeter (Molecular Devices). For $IC_{50}$ determination, the initial slope for each reaction was determined using a curve fitting function of the GraphPad Prism 5 program (GraphPad Software), and plotted as a function of compound concentrations. The slope in the absence of compound was set as "100% activity."

### NMR

All NMR spectra were recorded at 298 K on a Bruker Avance 600-MHz spectrometer equipped with a TXI cryoprobe. NMR samples were prepared in 0.4 ml of 99.9% $^2H_2O$ buffer containing 10 mM Tris-*d8*-$^2$HCl, pH 8.0, and 10 mM $MgCl_2$. Protein concentrations were 1 μM. CPYPP was dissolved in 99.96% DMSO-*d6* at 2 mg/ml, and added to the protein samples at a final concentration of 100 μM. STD NMR spectra were acquired with the pulse sequence as described (Mayer and Meyer, 2001). The on-resonance irradiation of the protein methyl signal region was set at a chemical shift of −0.2 ppm, and the off-resonance irradiation was set at −30 ppm, where no protein signals were present, with a total saturation time of 2 s. The suppression of the residual $^1H^2HO$ signal was achieved by the WATERGATE technique. The STD effect was verified by efficient cancellation of the impurity peaks.

### SPR-Based Binding Assays

SPR-based binding assays were performed using a Biacore T200 (GE Healthcare). His-SUMO-DOCK2$^{DHR\text{-}2\Delta lobeA}$ was immobilized on NTA Sensor Chip (GE Healthcare) with a covalent coupling of His-tagged protein to nitrilotriacetic acid (NTA) biosensor surface (Willard and Siderovski, 2006). NTA Sensor Chip was washed with 0.35 M EDTA for 60 s (10 μl/min) followed by extra wash with a buffer (10 mM HEPES, pH 7.4; 150 mM NaCl, 50 μM EDTA, 0.1% Tween 20). Then the chip was activated with 500 μM $NiCl_2$ for 60 s (10 μl/min) followed by extra wash with 3 mM EDTA. Finally, His-SUMO-DOCK2$^{DHR\text{-}2\Delta lobeA}$ was immobilized on the chip by amine coupling (Amine Coupling Kit, GE Healthcare) after injection of EDC (1-ethyl-3(3-dimethylaminopropyl)-carbodiimide hydrochloride)/NHS (10 μl/min, 7 min) and His-SUMO-DOCK2$^{DHR\text{-}2}$ (10 μl/min, 7 min), and deactivation with ethanol amine (10 μl/min, 7 min). We could capture significant amount of His-SUMO-DOCK2$^{DHR\text{-}2\Delta lobeA}$ (~3,000 RU) for affinity experiments. SPR measurements were carried out with a running buffer (10 mM HEPES, pH 7.4; 150 mM NaCl, 50 μM EDTA, 0.1% Tween 20, and 8% DMSO). For this purpose, compounds were diluted with the running buffer to keep DMSO concentration at 8%. Then the sample was injected for 60 s (contact phase), and 180 s of buffer flow (dissociation phase) was followed. The flow rate was set at 30 μl/min. For extra wash, 50% DMSO was used. The binding response (RU) of compounds to His-SUMO-DOCK2$^{DHR\text{-}2\Delta lobeA}$ was determined with the Biacore T200 evaluation software.

### Cell Preparation

pDCs were prepared from bone marrow (BM) cells using Flt3 ligand as described previously (Gotoh et al., 2010). T cells and B cells were isolated from spleen and lymph nodes using Pan-T cell isolation kit and B cell isolation kit (both from Myltenii Biotec), respectively. $CD4^+$ T cells were isolated by magnetic sorting with Dynabead Mouse CD4 followed by treatment with DETACHaBEAD Mouse CD4 (both from Dynal). Cell viability was determined with CytoTox 96 nonradioactive cytotoxicity assay (Promega) according to the manufacture's instructions.

### Rac Activation Assays

Before assays, cells were stimulated with CCL21 (1 μg/ml), CXCL13 (1 μg/ml), anti-CD3ε antibody (145-2c11; 10 μg/ml) followed by crosslinking with anti-hamster IgG (10 μg/ml), or CpG-A (3 μM). Aliquots of the cell extracts were kept for total lysate controls, and the remaining extracts were incubated with GST-fusion Rac-binding domain of PAK1 at 4°C for 60 min. The bound proteins and the same amounts of total lysates were analyzed by SDS-PAGE, and blots were probed with anti-Rac antibody (23A8, Millipore).

### Chemotaxis Assays

Transwell chemotaxis assays were performed using CCL21 (300 ng/ml) or CXCL13 (2 μg/ml) as a chemoattractant for T cells or B cells, respectively. After incubation for 2 hr at 37°C, spleen cells migrated to the lower chamber were collected, and stained for Thy1.2 and B220. The percentage of migrated cells was calculated by dividing the number of $Thy1.2^+$ cells (T cells) or $B220^+$ cells (B cells) in the lower chamber by the number of input cells.

### MLR

T cells ($3 \times 10^5$) from C57BL/6 mice were cultured with irradiated spleen cells ($1 \times 10^6$) from B10.BR or C57BL/6 mice in the presence of various concentrations of CPYPP or DMSO for 84 hr, and [$^3$H]-thymidine (0.037 MBq) was added during the final 16 hr of the culture. Cells were harvested on glass filter paper, and the incorporated radioactivity was measured with a liquid scintillation counter.

### Measurement of Cytokine Production

Flt3 ligand-induced BM-derived pDCs were stimulated with CpG-A (3 μM) for 24 hr in the presence of CPYPP or DMSO. Concentrations of IFN-α (R&D Systems) and IL-12p40 (Thermo Fisher Scientific) in cell-culture supernatants were measured by ELISA kit.

### In Vivo Homing Assays

Spleen cells ($1 \times 10^8$) isolated from DOCK2-GFP knock-in mice were transferred intravenously into C57BL/6 mice that had been treated intraperitoneally with 100 μl of CPYPP (50 mg/ml in DMSO) or intravenously with 50 μl of CPYPP (1 mg/ml in DMSO) 1 hr before the transfer. Mice were sacrificed 1 hr later, and cells were prepared from the spleen and the peripheral lymph nodes. Cells were then stained for CD3ε, and the percentages of migrated T cells were calculated.

### Measurement of Plasma Concentration of CPYPP

The plasma concentration of CPYPP was determined using LC-MS/MS (Prominence 2000 series liquid chromatography system, Shimadzu, coupled to an API-3000 mass spectrometer, Applied Biosystems). A CPYPP standard curve using 5 μl of serially diluted CPYPP in DMSO into 50 μl of plasma (final concentration range from 0.01 to 30 μg/ml) was used to determine CPYPP concentration in plasma. Following protein precipitation by acetonitrile containing 0.1 μg/ml of diazepam (internal standard), samples were cleared by centrifugation (15 min, 3,500 rpm, 4°C) and fractionated on a Capcell PAK C18 MG column (3 μm, 2.0 × 35 mm; Shiseido) at 50°C using a 0.1% formic acid/water to 0.1% formic acid/acetonitrile gradient with a flow rate of 0.3 ml/min. Detection of CPYPP and diazepam was carried out by positive electrospray ionization mode with transitions of m/z 325–164 and m/z 285–193, respectively. The ratio of chromatographic peak areas of CPYPP to diazepam was used to calculate the plasma CPYPP concentration and expressed as μM by unit conversion.

### Measurement of Intracellular CPYPP Content

An oil filtration assay was applied to determine relative intracellular accumulation of CPYPP by using Transporter Suspension Assay Kit (BD Biosciences). Microcentrifuge tubes from the kit were conditioned by addition of 100 μl of 2 N NaOH solution followed by layering filtration oil onto the NaOH solution. Spleen cells of BALB/c mice ($1 \times 10^7$/ml) were incubated in RPMI1640 medium supplemented with 0.5% BSA or 10% FCS in the presence or absence of 100 μM CPYPP. After 1 or 5 hr of incubation at 37°C, the splenocyte suspension in each culture media was loaded onto the oil layer and centrifuged (12,000 rpm, 30 s) to pellet cells in the NaOH layer, enabling quick wash and splenocyte collection. Splenocyte suspension in NaOH were taken off by scissoring microcentrifuge tube and aspirating the remaining oil, then incubated at 37°C for 10 min for solubilization. These samples were neutralized by HCl and diluted by acetonitrile with 0.1 μg/ml of diazepam. Samples were injected into the LC-MS/MS system to detect peak areas of CPYPP and diazepam. The ratio of peak areas of CPYPP to diazepam was used to compare intracellular content of CPYPP.

### Statistical Analysis

Statistical analyses were performed using one-way analysis of variance (ANOVA) followed by Dunnett's test (Figures 2D, 5B, 6C, 6D, 7B, and 7D) or two-tailed Student's t test (Figures 3D, 6A, 6B, 6E, 7A, and 7C). Analyses were done with GraphPad Prism 5 software.

## SUPPLEMENTAL INFORMATION

Supplemental Information includes six figures, one table, and Supplemental Experimental Procedures and can be found with this article online at doi:10.1016/j.chembiol.2012.03.008.

 

## ACKNOWLEDGMENTS

We thank A. Inayoshi and M. Sanematsu for technical assistance. This work was supported by grants for Targeted Proteins Research Program from the Ministry of Education, Culture, Sports, Science and Technology of Japan, Grants-in-Aid for Scientific Research from the Japan Society for the promotion of Science, CREST program of Japan Science and Technology Agency, the Kanae Foundation, the Mochida Memorial Foundation, and the Tokyo Biochemical Research Foundation.

Received: September 19, 2011
Revised: February 17, 2012
Accepted: March 1, 2012
Published: April 19, 2012

## REFERENCES

Anderson, M.S., and Bluestone, J.A. (2005). The NOD mouse: a model of immune dysregulation. Annu. Rev. Immunol. *23*, 447–485.

Blanco, P., Palucka, A.K., Gill, M., Pascual, V., and Banchereau, J. (2001). Induction of dendritic cell differentiation by IFN-α in systemic lupus erythematosus. Science *294*, 1540–1543.

Brinkmann, V., Billich, A., Baumruker, T., Heining, P., Schmouder, R., Francis, G., Aradhye, S., and Burtin, P. (2010). Fingolimod (FTY720): discovery and development of an oral drug to treat multiple sclerosis. Nat. Rev. Drug Discov. *9*, 883–897.

Brugnera, E., Haney, L., Grimsley, C., Lu, M., Walk, S.F., Tosello-Trampont, A.-C., Macara, I.G., Madhani, H., Fink, G.R., and Ravichandran, K.S. (2002). Unconventional Rac-GEF activity is mediated through the Dock180-ELMO complex. Nat. Cell Biol. *4*, 574–582.

Côté, J.-F., and Vuori, K. (2002). Identification of an evolutionarily conserved superfamily of DOCK180-related proteins with guanine nucleotide exchange activity. J. Cell Sci. *115*, 4901–4913.

Deacon, S.W., Beeser, A., Fukui, J.A., Rennefahrt, U.E.E., Myers, C., Chernoff, J., and Peterson, J.R. (2008). An isoform-selective, small-molecule inhibitor targets the autoregulatory mechanism of p21-activated kinase. Chem. Biol. *15*, 322–331.

Denton, M.D., Magee, C.C., and Sayegh, M.H. (1999). Immunosuppressive strategies in transplantation. Lancet *353*, 1083–1091.

Dustin, M.L., and Cooper, J.A. (2000). The immunological synapse and the actin cytoskeleton: molecular hardware for T cell signaling. Nat. Immunol. *1*, 23–29.

Faroudi, M., Hons, M., Zachacz, A., Dumont, C., Lyck, R., Stein, J.V., and Tybulewicz, V.L.J. (2010). Critical roles for Rac GTPases in T-cell migration to and within lymph nodes. Blood *116*, 5536–5547.

Fukui, Y., Hashimoto, O., Sanui, T., Oono, T., Koga, H., Abe, M., Inayoshi, A., Noda, M., Oike, M., Shirai, T., and Sasazuki, T. (2001). Haematopoietic cell-specific CDM family protein DOCK2 is essential for lymphocyte migration. Nature *412*, 826–831.

Gao, Y., Dickerson, J.B., Guo, F., Zheng, J., and Zheng, Y. (2004). Rational design and characterization of a Rac GTPase-specific small molecule inhibitor. Proc. Natl. Acad. Sci. USA *101*, 7618–7623.

Gerard, C., and Rollins, B.J. (2001). Chemokines and disease. Nat. Immunol. *2*, 108–115.

Gilliet, M., Cao, W., and Liu, Y.-J. (2008). Plasmacytoid dendritic cells: sensing nucleic acids in viral infection and autoimmune diseases. Nat. Rev. Immunol. *8*, 594–606.

Gotoh, K., Tanaka, Y., Nishikimi, A., Nakamura, R., Yamada, H., Maeda, N., Ishikawa, T., Hoshino, K., Uruno, T., Cao, Q., et al. (2010). Selective control of type I IFN induction by the Rac activator DOCK2 during TLR-mediated plasmacytoid dendritic cell activation. J. Exp. Med. *207*, 721–730.

Hall, A. (1998). Rho GTPases and the actin cytoskeleton. Science *279*, 509–514.

Jiang, H., Pan, F., Erickson, L.M., Jang, M.-S., Sanui, T., Kunisaki, Y., Sasazuki, T., Kobayashi, M., and Fukui, Y. (2005). Deletion of DOCK2, a regulator of the actin cytoskeleton in lymphocytes, suppresses cardiac allograft rejection. J. Exp. Med. *202*, 1121–1130.

Kulkarni, K., Yang, J., Zhang, Z., and Barford, D. (2011). Multiple factors confer specific Cdc42 and Rac protein activation by dedicator of cytokinesis (DOCK) nucleotide exchange factors. J. Biol. Chem. *286*, 25341–25351.

Luster, A.D., Alon, R., and von Andrian, U.H. (2005). Immune cell migration in inflammation: present and future therapeutic targets. Nat. Immunol. *6*, 1182–1190.

Mandala, S., Hajdu, R., Bergstrom, J., Quackenbush, E., Xie, J., Milligan, J., Thornton, R., Shei, G.-J., Card, D., Keohane, C., et al. (2002). Alteration of lymphocyte trafficking by sphingosine-1-phosphate receptor agonists. Science *296*, 346–349.

Mayer, M., and Meyer, B. (2001). Group epitope mapping by saturation transfer difference NMR to identify segments of a ligand in direct contact with a protein receptor. J. Am. Chem. Soc. *123*, 6108–6117.

Meller, N., Irani-Tehrani, M., Kiosses, W.B., Del Pozo, M.A., and Schwartz, M.A. (2002). Zizimin1, a novel Cdc42 activator, reveals a new GEF domain for Rho proteins. Nat. Cell Biol. *4*, 639–647.

Meyer, B., and Peters, T. (2003). NMR spectroscopy techniques for screening and identifying ligand binding to protein receptors. Angew. Chem. Int. Ed. Engl. *42*, 864–890.

Nestle, F.O., Conrad, C., Tun-Kyi, A., Homey, B., Gombert, M., Boyman, O., Burg, G., Liu, Y.-J., and Gilliet, M. (2005). Plasmacytoid predendritic cells initiate psoriasis through interferon-α production. J. Exp. Med. *202*, 135–143.

Nishikimi, A., Fukuhara, H., Su, W., Hongu, T., Takasuga, S., Mihara, H., Cao, Q., Sanematsu, F., Kanai, M., Hasegawa, H., et al. (2009). Sequential regulation of DOCK2 dynamics by two phospholipids during neutrophil chemotaxis. Science *324*, 384–387.

Nombela-Arrieta, C., Lacalle, R.A., Montoya, M.C., Kunisaki, Y., Megías, D., Marqués, M., Carrera, A.C., Mañes, S., Fukui, Y., Martínez-A, C., and Stein, J.V. (2004). Differential requirements for DOCK2 and phosphoinositide-3-kinase γ during T and B lymphocyte homing. Immunity *21*, 429–441.

Nombela-Arrieta, C., Mempel, T.R., Soriano, S.F., Mazo, I., Wymann, M.P., Hirsch, E., Martínez-A, C., Fukui, Y., von Andrian, U.H., and Stein, J.V. (2007). A central role for DOCK2 during interstitial lymphocyte motility and sphingosine-1-phosphate-mediated egress. J. Exp. Med. *204*, 497–510.

Reif, K., and Cyster, J.G. (2002). The CDM protein DOCK2 in lymphocyte migration. Trends Cell Biol. *12*, 368–373.

Sanui, T., Inayoshi, A., Noda, M., Iwata, E., Oike, M., Sasazuki, T., and Fukui, Y. (2003). DOCK2 is essential for antigen-induced translocation of TCR and lipid rafts, but not PKC-θ and LFA-1, in T cells. Immunity *19*, 119–129.

Shulman, Z., Pasvolsky, R., Woolf, E., Grabovsky, V., Feigelson, S.W., Erez, N., Fukui, Y., and Alon, R. (2006). DOCK2 regulates chemokine-triggered lateral lymphocyte motility but not transendothelial migration. Blood *108*, 2150–2158.

Shutes, A., Onesto, C., Picard, V., Leblond, B., Schweighoffer, F., and Der, C.J. (2007). Specificity and mechanism of action of EHT 1864, a novel small molecule inhibitor of Rac family small GTPases. J. Biol. Chem. *282*, 35666–35678.

Tybulewicz, V.L.J., and Henderson, R.B. (2009). Rho family GTPases and their regulators in lymphocytes. Nat. Rev. Immunol. *9*, 630–644.

Vicente-Manzanares, M., and Sánchez-Madrid, F. (2004). Role of the cytoskeleton during leukocyte responses. Nat. Rev. Immunol. *4*, 110–122.

Villalba, M., Bi, K., Rodriguez, F., Tanaka, Y., Schoenberger, S., and Altman, A. (2001). Vav1/Rac-dependent actin cytoskeleton reorganization is required for lipid raft clustering in T cells. J. Cell Biol. *155*, 331–338.

Willard, F.S., and Siderovski, D.P. (2006). Covalent immobilization of histidine-tagged proteins for surface plasmon resonance. Anal. Biochem. *353*, 147–149.

Yang, J., Zhang, Z., Roe, S.M., Marshall, C.J., and Barford, D. (2009). Activation of Rho GTPases by DOCK exchange factors is mediated by a nucleotide sensor. Science *325*, 1398–1402.

Yu, H., Leitenberg, D., Li, B., and Flavell, R.A. (2001). Deficiency of small GTPase Rac2 affects T cell activation. J. Exp. Med. *194*, 915–926.

  